

---

# 9 Toward BCIs Out of the Lab

## *Impact of Motion Artifacts on Brain–Computer Interface Performance*

*Ana Matran-Fernandez, Davide Valeriani, and Riccardo Poli*

### CONTENTS

9.1	Introduction .....	220
9.1.1	Brain–Computer Interfaces .....	220
9.1.2	Artifacts and Their Effects on BCIs.....	220
9.1.3	Artifact Correction and Rejection and Their Limitations .....	221
9.1.4	Contributions of This Study .....	222
9.2	Data Collection .....	223
9.2.1	BCI Data .....	223
9.2.2	Artifacts .....	224
9.3	Data Processing and Classification.....	226
9.3.1	Preprocessing BCI Data.....	226
9.3.2	Preprocessing Artifacts .....	226
9.3.3	Creation of Simulated Portable BCI Data Sets.....	226
9.3.4	Feature Extraction .....	227
9.3.5	Classification.....	229
9.4	Results.....	230
9.4.1	Baseline.....	230
9.4.2	Performance on Simulated Portable BCI Data Sets .....	230
9.4.3	Effects of Training with Simulated Portable BCI Data Sets .....	233
9.5	Conclusions and Future Work.....	235
	References.....	236

## 9.1 INTRODUCTION

### 9.1.1 BRAIN–COMPUTER INTERFACES

A brain–computer interface (BCI) is a system that provides a direct pathway between the brain and an external device, allowing people to act on the world without moving any muscle. In order to do so, the BCI needs access to the central nervous system and, in particular, to the brain. Invasive BCI systems are those that are implanted directly into the brain of the user [1,2]. They allow the detection of cleaner signals, but they need surgery to be installed. On the other hand, in noninvasive BCIs, the insight into the neural processes is most frequently given by electroencephalography (EEG) systems that record the electric activity of the brain from the scalp of the user [3–15]. EEG-based BCIs have several advantages: they are easy to use, are compact, and provide a very good time resolution. Thanks to these, several applications have been suggested in the last decades for EEG-based BCIs.

Initially EEG-based BCIs were developed as tools to enhance the quality of life of people with severe motor disabilities (e.g., locked-in) [12,16]. In this application, the main focus is to provide systems that are reliable, efficient, and easy to use in a real context, which includes their portability. They have also been used as passive tools for able-bodied users (e.g., for monitoring driver’s attention levels in a car or as an extra input to control a videogame) [17,18]. Moreover, if the EEG recording system is discreet enough, portable BCIs could be conceived as a wearable device, for monitoring changes in brain activity through the day [19]. Indeed, EEG recordings are also routinely used for medical applications, for example, for the characterization of epileptic seizures and study of sleep and brain lesions [20–22].

While until very recently all BCIs involved an individual user, collaborative BCIs (i.e., BCIs that are used simultaneously by several users to control one device) have now started to show their advantages in speed and accuracy with respect to non-BCI users and single-user BCIs. There are indications that, in the future, they could be adopted for use in the workplace, for example, by intelligence analysts [23,24] or in group decision making [25].

### 9.1.2 ARTIFACTS AND THEIR EFFECTS ON BCIs

Despite all the advantages of these noninvasive BCIs, they also present a major drawback associated with the nature of EEG: the neural signals recorded from the scalp are highly affected by a variety of artifacts [26,27]. These include the electrical activity of the heart (electrocardiogram), inconsistent contact of the electrodes, (for example, because of movements), and muscle artifacts (electromyogram [EMG]) such as those induced by neck movements, ocular activity (electrooculogram [EOG]), eye blinks, swallowing, and so on. These artifacts can affect the quality of the EEG signals recorded, consequently deteriorating the performance of the BCI system.

EOG artifacts, for instance, may be orders of magnitude bigger than the ordinary elements of EEG. Therefore, when they are present in the recording, it is usually impossible to detect the small variations of the voltages that represent the brain processes. EOG artifacts can also lead to extremely larger deviations from the desired

behavior in BCIs, particularly those where there is an analog relationship between input signals and output control signals, such as in the Essex BCI Mouse [15,28,29].

For these reasons, the control of artifacts is a very important step in BCI research.

### 9.1.3 ARTIFACT CORRECTION AND REJECTION AND THEIR LIMITATIONS

Fundamentally, there are two approaches one can take to deal with artifacts: *correction* and *rejection* [27,30].

Correction means subtracting out the effects of the artifacts from the EEG signal. This requires estimating the contribution of the artifacts on the recorded signal. For example, the effects of eye blinks and vertical components of saccades can be reduced by using the time-domain linear regression between each channel and the vertical EOG [27,31], by using dipole localization procedures [32], or by applying independent component analysis (ICA) [33] to decompose EEG signals into independent components (sources variability) and subtract from the EEG those that represent pure artifacts [34–38]. EMG artifacts could be removed by applying a low-pass filter to the EEG signal or by using ICA or regression methods [30,39].

However, while the correction technique is well used in literature to deal with EOG artifacts, its application to other sources of noise is not straightforward. Many more types of artifacts are not only possible but ubiquitous if the EEG is recorded outside the laboratory (for example, for utilization in a portable BCI). Under laboratory conditions, experimenters usually ask the volunteers to hand over their mobile phones to avoid noise from electrical devices, and the instructions given in the protocol ask them to remain as still as possible, try to avoid eye blinks, and so on. While these measures are widely accepted in event-related potential (ERP) studies, they are not realistic for the daily use of a BCI.

Moreover, despite the wide use of artifact correction methods, some skepticism remains as to whether these are actually introducing distortions in the corrected EEG data [32]. In order to validate an artifact correction method, one would have to first contaminate data and then show how the corrected data compare to the original signal before contamination.

The second approach is rejection, where fragments of EEG (or trials) affected by artifacts are simply removed from the analysis. Rejection requires the *detection* of artifacts (while correction does not necessarily require it). For instance, two of the simplest and fastest automated detectors for EOG artifacts are as follows [27,40]: (a) deleting portions of the data where the EOG amplitude deviates by more than a set threshold, say, 50  $\mu\text{V}$  or 75  $\mu\text{V}$ , from the baseline; (b) measuring the difference,  $\Delta V$ , between the maximum and minimum EOG amplitude within a block of the signal and rejecting it if  $\Delta V$  exceeds a threshold.

Artifact detectors usually require positioning some extra electrodes on the subject (e.g., around the eyes for EOG detection), making the BCI system less portable. Although there are a number of effective techniques to detect and remove artifacts (e.g., see Refs. [38,41] for EOG) without the availability of these extra electrodes, they are quite complex, especially considering that they should be applied for various types of artifacts that could affect the EEG signal.

Beyond the system's complexity, the main disadvantage of artifact rejection is that it can significantly reduce the amount of epochs available for ERP analysis [32]. In the BCI field, discarding epochs that contain artifacts would slow down the performance of the BCI. Depending on the percentage of discarded trials, this might not be acceptable for the user. For this reason, since various artifacts can affect the same EEG signal, not all contaminated trials can be rejected and, therefore, the rejection approach is usually not sufficient to get "clean" signals.

Therefore, it is unlikely to be able to rely on EEG signals that are not affected by noise in an EEG-based portable BCI system. If we first focus on the utilization of a portable BCI by a disabled person, even in the case of he or she being completely locked-in, the environment will introduce noise in the EEG signals that should be processed by the system. In this extreme case, it is important that the BCI is built so that its performance is not significantly affected by such interference. In the case of able-bodied users, the main sources of noise will probably be motion artifacts, and it is thus important to know which types of artifacts will be more likely to affect performance and how robust a BCI can be with respect to them.

#### 9.1.4 CONTRIBUTIONS OF THIS STUDY

To start assessing how close we are to performing a transition from the laboratory (with seated and static users and noise- and distraction-free environments) to the real world (which is noisy, dynamic, and distracting, and in which users constantly move and perform other actions besides controlling a computer with their brains), in this chapter we studied the impact of several types of artifacts on the performance of a BCI. In particular, we wanted to see whether the trained classifier that virtually all modern BCIs include could cope with the artifacts.

More specifically, in the following, we will analyze the impact of more than 20 different types of artifacts on a portable EEG-based BCI system. Instead of dealing with artifact rejection or correction, considering the limitations described above, our aim is to investigate to what degree a portable BCI applied to everyday life can still adequately perform in comparison to a BCI used under laboratory conditions and in the absence of noise and artifacts. By considering this high number of different types of artifacts, we may be able to figure out which of those have a high impact on the performance of the portable BCI system and, on the other hand, for which ones the system is robust enough to ignore them. Relatively little is known about how much the performance of a portable BCI would be affected by such a wide range of artifacts.

The analysis will focus on the artifacts that reflect movements that are typical in a driving scenario. Apart from the "classical" artifacts (like eye movements and eye blinks), actions like moving the head or changing the gear with one hand will also be included. We chose a driving scenario since many possible applications of BCI systems are in the automotive area [42]. The Essex BCI Mouse has been shown to be suitable for control of a spaceship in a videogame [43]. It is possible to envision a system in which a similar controller can be embedded on the windscreen of a car, in a way that allows for brain control while driving. Also, portable BCI systems could be integrated in a car to monitor the level of attention of the driver and raise an alarm

in case of danger, in order to reduce the possibility of accidents. However, one of the main limitations of this application is precisely the large amount of noise generated by the movements performed by the driver while he or she is driving. This is the scenario on which we focus for the rest of the chapter.

While this serves as a good framework for a first approach to the topic of portable BCI, it has obvious limitations. For example, we do not study here walking-derived artifacts, which of course cannot be applied in a driving task. However, the conclusions of this study can be applied not only to driving scenarios but also for wheelchair users, gamers, and, in general, any other BCI application in which the able-bodied user of the BCI performs a task while remaining seated.

Moreover, this study contributes to bringing BCI out of the laboratory. The conclusions drawn about the impact of different types of artifacts could be used for portable BCI applications, such as wearable devices, to reduce the complexity of the system, focusing the processing mechanisms for artifact correction on those types that affect BCI performance most severely.

The chapter has the following structure. Section 9.2 describes the protocol we used to record the neural data in the original BCI protocol and the data used to add different artifacts to it. Section 9.3 describes the methodology applied to process, classify, and analyze the data. In Section 9.4, we show and discuss the results obtained with the clean and the artifact-contaminated data sets. Finally, in Section 9.5 we draw some conclusions about this work and include suggestions for further work.

## 9.2 DATA COLLECTION

This section will focus on describing how the neural data were collected. As we mentioned in Section 9.1, rather than utilizing data from a portable BCI, we artificially added artifacts to BCI data collected under laboratory conditions in previous experiments and studied the effects of this added noise on BCI performance. We will begin by describing the BCI data (i.e., data acquired during a real BCI experiment) and will then continue with an explanation of the protocol that we followed to collect new data containing different types of artifacts.

In both cases, data were acquired with a BioSemi ActiveTwo EEG system. Neural data were recorded from 64 electrode sites (see [Figure 9.4](#)), organized according to the 10–20 system, and referenced to the mean of the electrodes placed on both earlobes.

### 9.2.1 BCI DATA

In the present study, we used a subset of the data gathered from 16 participants (average age of 30, all with normal or corrected to normal vision except for one who had strabismus with exotropia in the left eye) in the two experiments reported in Ref. [14], where a variety of visual stimulation protocols to be used in a BCI mouse were tested.

As illustrated in [Figure 9.1](#), in the experiments, participants were presented with a display containing eight circles (with each circle representing a direction of movement for the mouse cursor) that formed an imaginary circle at the center of the display. The circles (stimuli) flashed sequentially (by changing rapidly from a baseline color to a different color and back) for 100 ms each without any delays in between.

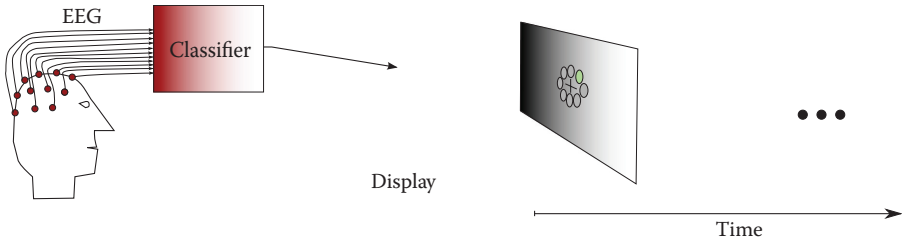


**FIGURE 9.1** Stimulation protocol used in our BCI mouse.

This meant that all eight different stimuli from the imaginary circle flashed within 800 ms, forming what we call a *circle epoch*.

The experiments were divided into runs, which we call *direction epochs*. Each direction epoch contained between 20 and 24 circle epochs and, thus, lasted between 16 and 19.2 s.

At the beginning of each direction epoch, participants were assigned a target circle and asked to perform the task of mentally naming its color every time it flashed. As we will detail below, the flashing of a circle constitutes the beginning of a *trial epoch*. If the flashed circle was the target circle, the trial epoch was labeled as a *target*. Otherwise, it was labeled as a *nontarget*.

Each participant carried out 16 direction epochs, with each circle being a target in two of them.

## 9.2.2 ARTIFACTS

As we indicated above, in this chapter, we will be focusing on BCIs that are controlled while the user is driving a car. Hence, we chose a pool of possible actions that are typically performed while driving. This activity involves doing several different actions, such as looking at side mirrors or changing the gear, that could generate artifacts in the EEG recording.

More specifically we decomposed it into 24 different activities representing eye, face, neck, arm, and leg movements. The complete list comprises turn/bend neck to the left/right, move head up/down, move eyes up/down/to the left/to the right, move tongue with the mouth closed, blink once/repeatedly, turn the wheel left/right, change gear with left/right hand, yawn, swallow, count in loud voice, cross left (respectively, right) foot over right (respectively, left), squint, and a baseline “do nothing” condition. Some of these activities have been depicted in [Figure 9.2](#).

To generate artifactual EEG signals, we asked a volunteer (27-year-old female) to perform the 24 actions (one at a time) while we were recording her brain activity. She was asked to perform 15 repetitions of each action, for a total of 360 trials. The order in which these were performed was randomized.

The protocol used was as follows. The participant was presented with a display showing a black screen. The screen then showed the name of the task (written as in [Figure 9.2](#)). To avoid ERPs and neural activity related to the processing of the task, the participant was asked to wait for 1 s after the onset of the task before performing

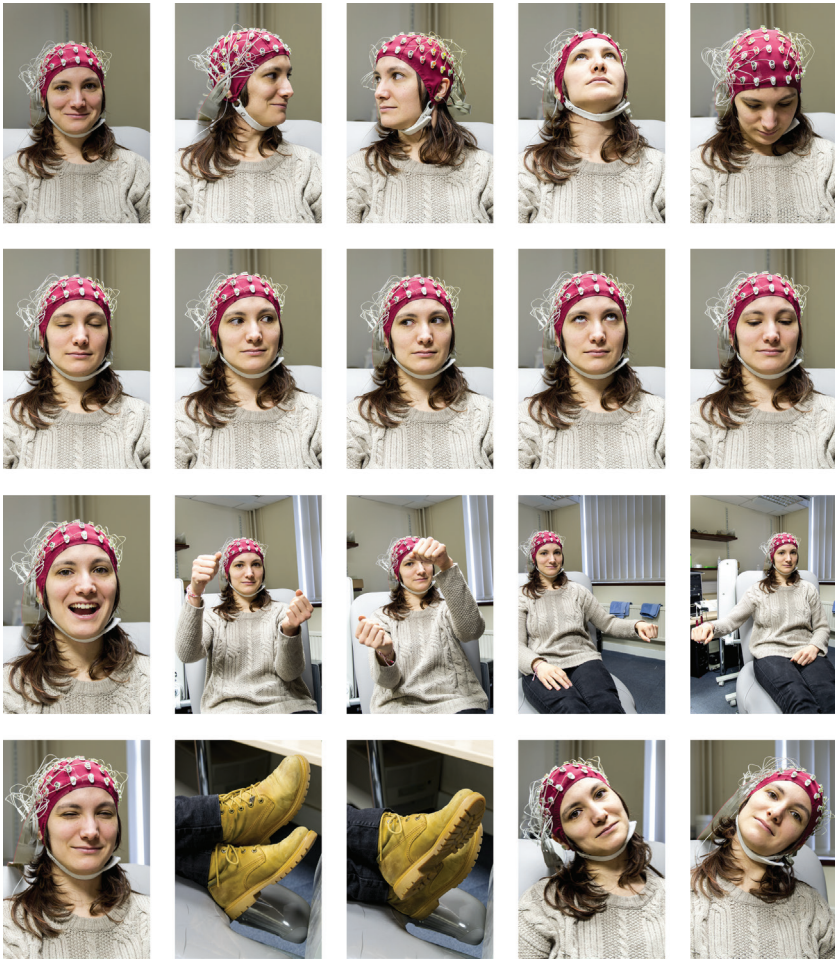


**FIGURE 9.2** Movements performed to generate noise. From top left to bottom right: do nothing, turn neck to the left, turn neck to the right, move head up, move head down, blink, move eyes to the left, move eyes to the right, look up, look down, yawn, turn the wheel left, turn the wheel right, change gear with the left hand, change gear with the right hand, squint, cross right foot over left, cross left foot over right, bend neck to the right, bend neck to the left.

the required action. She then had a 3-s time window to perform the action. Five seconds after the onset of task presentation, the screen turned black again and stayed static until the participant indicated, through the press of a mouse button, that she was ready to move for the next task.

The volunteer was seated on an electrically adjustable chair that had been unplugged from the mains to prevent it from injecting electromagnetic noise in the EEG data. After the recording of the 24 types of movements, she was asked to remain still (the screen showed the “do nothing” instruction) while the chair was reconnected to the mains. An extra 15 trials were recorded in this scenario.

### 9.3 DATA PROCESSING AND CLASSIFICATION

We begin this section by describing the preprocessing stage for both the BCI data and the epochs containing artifacts. We then describe the way in which we blended the signals from the two protocols to generate artifact-contaminated BCI data. We end the section with a description of our classification approach, including our methods for electrode optimization and performance assessment.

#### 9.3.1 PREPROCESSING BCI DATA

The EEG data from the BCI mouse experiment were initially collected at a sampling rate of 2048 Hz, band-pass filtered between 0.15 and 40 Hz, and finally down-sampled to 512 Hz.

From each channel (or electrode), an 800-ms trial epoch starting at the flashing of a circle was extracted and further decimated (with averaging) to a sampling frequency of 12.5 Hz. Therefore, a trial epoch was represented by 10 samples per channel. If the flashed circle had been identified as the target of the direction epoch, that trial epoch was labeled as a target epoch, whereas nontarget epochs were those that started with the flashing of a nontarget circle.

Since the nontarget trials were much more frequent than the target ones (7 out of every 8 trials were nontargets), we balanced the two classes by randomly subsampling the nontarget trials on a participant-by-participant basis, in order to improve the performance of the classifier.

The data sets created from these data will be referred to in the rest of the chapter as  $D_0$ .

#### 9.3.2 PREPROCESSING ARTIFACTS

For each trial, we extracted an artifact epoch starting 1 s after the presentation of the task and lasting 3 s.

As before, also artifact epochs were referenced to the mean of all EEG channels and to the mean of the earlobes, band-pass filtered between 0.15 and 40 Hz and downsampled by a factor of 4, to the final sampling rate of 512 Hz.

Since these artifacts were added to “clean” BCI data from a different experiment, we then detrended each trial to ensure that the beginning and end of the epochs were 0 and, thus, no discontinuities were introduced in the BCI data when adding an artifact.

One to three detrended artifact epochs were then added to the BCI data at random positions in each direction epoch (more on this in Section 9.3.3).

#### 9.3.3 CREATION OF SIMULATED PORTABLE BCI DATA SETS

In order to determine the impact of different types of artifacts on a BCI, we created a number of simulated portable BCI data sets, each of which consisted of “noisy” epochs  $Ep_{i,j,k}$  for each participant of the BCI mouse experiment, where  $i \in \{1, \dots, 16\}$  is the direction epoch from which the BCI data are extracted,  $j \in \{1, \dots, 25\}$  is the

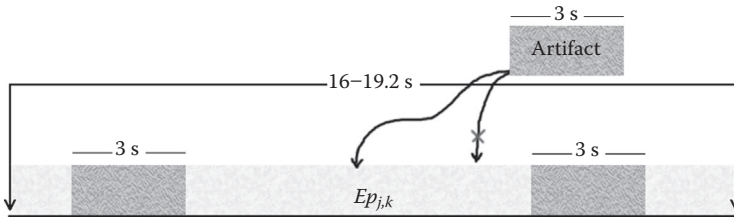


**FIGURE 9.3** Process of creation of  $Ep_{j,k}$ .

type of artifact that has been added to the neural data, and  $k \in \{1,2,3\}$  is the number of occurrences of that type of artifact in each direction epoch.\*

Each channel of  $Ep_{i,j,k}$  is obtained by adding a direction epoch extracted from the BCI data ( $Ep_i$ ) and a new epoch, which we call  $Ep_{j,k}$ , of the same length as  $Ep_i$ , which contains  $k$  artifact epochs from the new signals recorded from our volunteer. That is,

$$Ep_{i,j,k} = Ep_i + Ep_{j,k}. \tag{9.1}$$

The process of creation of  $Ep_{j,k}$  is depicted in Figure 9.3. First of all, a new structure of the same length of  $Ep_i$  is created and filled with 0's. Second,  $k$  random artifact epochs from the pool of 15 of type  $j$  are selected. These are added to the newly generated structure at random locations with the condition that no more than one artifact could be present at each sample.

In order to have data that are consistent, each channel of the recorded artifact was added to the corresponding channel of the BCI data. That is, each generated channel of  $Ep_{i,j,k}$  contains the summation of BCI data from that channel and  $k$  randomly placed artifacts as read on the same electrode site.

Finally, after the creation of  $Ep_{j,k}$ , this structure is added to a given run of the BCI mouse data ( $Ep_i$ ) before extracting and preprocessing the individual 800-ms trial epochs that are used for classifying trials.

Since we add between one and three 3-s artifact epochs to direction epochs lasting between 16 and 19.2 s, the percentage of contamination in the data sets ranges from 15%–19% (depending on the length of a direction epoch) for  $k = 1$  to 47%–56% for  $k = 3$ .

The procedure described above creates a total of 75 data sets for the simulated portable BCI. We will term each of these  $D_{j,k}$ , where, as above,  $j$  is the type of artifact that has been used to contaminate the original BCI data set and  $k$  is the number of artifact epochs added to a direction epoch.

### 9.3.4 FEATURE EXTRACTION

Various features have been used in BCI research to extract meaningful information from the EEG signal and improve the classification performance. In order to capture as

\* Since the epochs extracted and preprocessed from the artifact experiment (3 s) are much shorter than those of a direction epoch of the BCI mouse ( $Ep_i$ , between 16 and 19.2 s as described in Section 9.2.1), it is possible to have multiple artifacts occurring within a run. This allowed us to investigate the effect of different levels of contamination in the BCI.

much information as possible, we used an *optimal subset* of the EEG signals recorded from the 64 electrode sites as neural features that were given to the classifiers.

The process of choosing the best subset of channels was composed of two steps: *feature reduction* and *feature selection*.

First, we performed a feature reduction step to reduce the number of electrodes to be considered for the optimization process. We randomly split the original BCI data set into a training set (80%) and a test set (20%), keeping the same proportion of target and nontarget trials as in the original data set  $D_0$ . Then, we normalized both sets by subtracting the mean value and dividing by the standard deviation of the training set. The test set was kept separate for later use (described in Section 9.3.5) while we used a five-fold cross-validation loop on the training set to train and validate a Fisher discriminant analysis (FDA) classifier that used all possible combinations of subsets of electrodes as features. We then used the area under the curve (AUC) of the receiver operator characteristics (ROC) to rank the different subsets. The AUC is a well-known summary for ROC curves that has been used widely in machine learning—more on this in Section 9.3.5. By looking at each best subset of electrodes of each participant, we manually selected the electrodes that appeared in the best set at least in seven out of the eight volunteers. These were the electrode sites O2, PO8, Cz, PO4, PO7, PO3, Pz, Oz, and P8 shown in Figure 9.4. These electrodes cover the area where the P300 ERP is most easily detected.

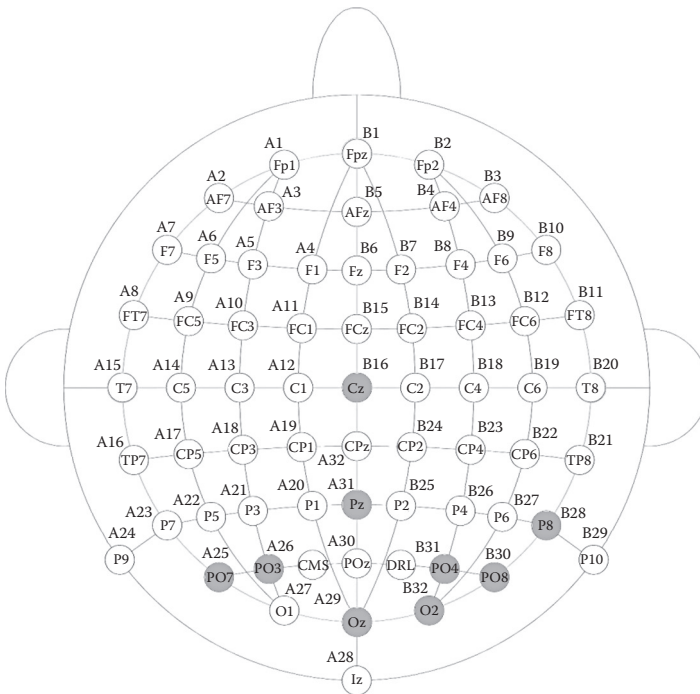


**FIGURE 9.4** The electrodes available in our EEG acquisition system. The gray locations represent the electrodes selected after feature reduction.

Second, we used this optimal set as a pool of electrodes in the *feature selection* step that was common for all participants. Then, using the training set from either the original  $D_0$  data set or the simulated portable BCI data sets, we tested all the possible subsets of between three and nine electrodes to find the best combination of features for each participant and type of data set using a five-fold cross-validation loop. The features from the optimal sets of electrodes found in this way were then used to train individually tailored classifiers, as we will explain in detail in Section 9.3.5.

### 9.3.5 CLASSIFICATION

In order to classify the features extracted from  $D_0$  and the artifact-contaminated data sets into the target and nontarget classes, we relied again on the FDA classifier, since it is frequently used in BCI research and it is efficient for real-time portable BCI use.

First, for each participant ( $p = 1, \dots, 8$ ), we used the optimal subset of electrodes that had been derived as described in Section 9.3.4 to extract features from the training set of  $D_0$ . These were used to train a classifier  $C_p$  that was specific for each participant, as is commonly done in BCI.

Then, we used the trained  $C_p$  to predict the classes (target versus nontarget) of the unseen trial epochs from the test sets of  $D_0$  and  $D_{j,k}$  (the original BCI data set and the simulated portable BCI data sets, respectively). Results from this first experiment are reported in Sections 9.4.1 and 9.4.2.

After training, the output of the FDA classifier can be interpreted as a measure of how closely the feature vector associated with the stimulus matches the target. By applying a threshold to this measure, one can transform it into a binary decision regarding the presence of a target. Naturally, the higher the threshold is, the less likely a false-positive error will be. However, unavoidably, a higher specificity brings a lower sensitivity (i.e., an increased number of false negatives) with it.

The behavior of our classifiers in relation to changes in their thresholds can be well represented using ROC curves. These are plots of the true-positive versus the false-positive rate for a binary classifier as its discrimination threshold is varied.

To measure the performance of  $C_p$  on each of the two data sets, we used the AUC of the classifier output. However, these results can be biased in favor of the original BCI data, since the classifiers were derived from training data from  $D_0$ . Indeed, the addition of artifacts to create  $D_{j,k}$  affects the features extracted and, consequently, can obscure the useful information that was originally available to the classifier when it derived a rule for predicting the label of a trial epoch. Moreover, the best set of electrodes found for the original BCI data set could be different from those found for the portable BCI data set (e.g., if the optimal subset of electrodes is calculated *after* adding the noise, the feature selection step will try to avoid selecting electrodes that are heavily affected by it).

Therefore, we augmented our analysis by training a number of classifiers  $C_{p,j,k}$  with the training set (generated as described in Section 9.3.4) of the simulated portable BCI data sets, where the subscripts have the same meaning as above. For each of these, an optimal subset of three to nine electrodes was derived before training the classifiers.

Finally, we used each  $C_{p,j,k}$  to predict the classes of the trials in the associated test set and the AUC to measure the performance. The results of this analysis are reported in Section 9.4.3.

## 9.4 RESULTS

### 9.4.1 BASELINE

In order to measure the extent to which a certain type of artifact affects the BCI, we first need to assess its performance under ideal laboratory conditions.

Table 9.1 shows the AUCs obtained using, for each classifier  $C_p$ , the training and test sets of participant  $p \in [1,8]$  extracted from the BCI mouse data set  $D_0$ .

We can observe that, with the approach described above, we achieved lower AUC values than those reported in Ref. [14]. This is reasonable since we used a lower number of features and a less complex classifier (FDA instead of a linear support vector machine) than the original research, in order to simplify the BCI system. However, in this chapter, we focus on the differences in performance between original and artifact-contaminated data sets, and not on the absolute performance of the BCI system.

### 9.4.2 PERFORMANCE ON SIMULATED PORTABLE BCI DATA SETS

After measuring the performance of our BCI under ideal laboratory conditions, we simulated the case in which one would train the classifier with data collected in the laboratory, in nearly ideal conditions, and then test the portable BCI out of the

---

**TABLE 9.1**  
**AUC Values Obtained by Our BCI**  
**for Each Participant for Target**  
**versus Nontarget Classification**

Participant	AUC
1	0.806
2	0.747
3	0.786
4	0.824
5	0.774
6	0.778
7	0.843
8	0.849
Mean	0.801
Median	0.796

*Note:* The last rows report the mean and median values across all participants.

---

laboratory. For this, we used the same classifiers  $C_p$  developed in Section 9.4.1 but calculated the AUC on the simulated portable BCI data sets ( $D_{j,k}$ ).

In this way, we can study the effects that each type of noise has on the performance of the BCI. The results of this analysis are collected in Table 9.2, where each value represents the median AUC across the individual classifiers  $C_p$  when testing on data from participant  $p \in [1,8]$  from the data set  $D_{j,k}$ . The numbers in brackets

**TABLE 9.2**  
**Performance of the BCI When Trained with Trials from  $D_0$  and Tested on Epochs from  $D_{j,k}$**

Noise Type	$k = 1$	$k = 2$	$k = 3$	Rank
Turn neck to the left	0.775 (0.117)	<b>0.716</b> (0.003)	<b>0.706</b> (0.000)	22
Turn neck to the right	0.763 (0.065)	<i>0.761</i> (0.025)	<i>0.741</i> (0.010)	20
Move head up	<i>0.747</i> (0.019)	<b>0.736</b> (0.002)	<b>0.686</b> (0.000)	25
Move head down	0.769 (0.065)	<b>0.715</b> (0.001)	<b>0.692</b> (0.001)	24
Move your tongue (mouth closed)	0.780 (0.323)	<i>0.759</i> (0.025)	<i>0.753</i> (0.032)	12
Move eyes to the left	0.766 (0.065)	<i>0.768</i> (0.032)	<i>0.769</i> (0.025)	8
Blink once	0.786 (0.439)	0.745 (0.080)	<i>0.768</i> (0.014)	10
Blink repeatedly	0.793 (0.287)	<i>0.768</i> (0.014)	<i>0.763</i> (0.032)	2
Move eyes to the right	0.774 (0.139)	0.762 (0.080)	<i>0.752</i> (0.025)	13
Look up	0.785 (0.334)	0.758 (0.052)	<b>0.739</b> (0.002)	17
Look down	0.778 (0.253)	0.761 (0.052)	<i>0.731</i> (0.019)	18
Turn the wheel left	0.773 (0.171)	0.776 (0.097)	<b>0.752</b> (0.007)	9
Turn the wheel right	0.784 (0.191)	<i>0.761</i> (0.010)	<i>0.743</i> (0.019)	15
Change gear with left hand	0.785 (0.171)	0.775 (0.080)	<i>0.756</i> (0.041)	5
Change gear with right hand	0.793 (0.221)	0.766 (0.117)	<b>0.747</b> (0.007)	7
Do nothing	0.789 (0.323)	<i>0.763</i> (0.032)	0.773 (0.080)	1
Yawn	0.786 (0.253)	<i>0.750</i> (0.014)	<b>0.747</b> (0.005)	16
Swallow	0.772 (0.080)	<i>0.761</i> (0.035)	<b>0.758</b> (0.007)	11
Count in loud voice	0.784 (0.360)	0.774 (0.065)	<i>0.764</i> (0.032)	3
Cross left foot over right	0.780 (0.262)	<b>0.749</b> (0.005)	<i>0.758</i> (0.032)	14
Cross right foot over left	0.780 (0.191)	<i>0.756</i> (0.019)	<b>0.730</b> (0.003)	19
Squint	0.787 (0.287)	0.765 (0.080)	<i>0.755</i> (0.032)	6
Bend neck to the right	0.775 (0.052)	<b>0.715</b> (0.000)	<b>0.696</b> (0.000)	23
Bend neck to the left	0.765 (0.065)	<b>0.735</b> (0.003)	<b>0.726</b> (0.000)	21
Electrical noise	0.778 (0.145)	<i>0.772</i> (0.032)	<i>0.769</i> (0.032)	4
Mean	0.778	0.755	0.743	

*Note:* Each number represents the median AUC across all participants for a specific type of artifact (from top to bottom,  $j = 1, \dots, 25$ ) and the given number of occurrences ( $k = 1, \dots, 3$ ). The last row represents the average AUC across data sets  $D_{j \in [1,25],k}$ . Numbers in parentheses represent the  $p$  values of a one-sided Wilcoxon test comparing BCI performance of classifiers  $C_p$  when tested on  $D_0$  versus the same classifiers tested on  $D_{j,k}$ . Numbers in italics represent statistical significance at the 5% confidence level. Numbers in boldface represent statistical significance at the 1% confidence level. The last column represents the ranking table (low numbers represent higher AUCs) determined by the mean value across columns  $k = 1, 2, 3$ .

represent the  $p$  values of a one-sided Wilcoxon test comparing BCI performance of classifiers  $C_p$  when tested on  $D_0$  versus the same classifiers tested on  $D_{j,k}$ .

Figure 9.5 shows examples of real trial epochs (*after* preprocessing) extracted from  $D_0$  (blue line) and corresponding artifact-contaminated epochs from  $D_{j,k}$  (black line). In this figure, we represent the effects of different types of artifacts that are approximately at the 90th percentile (“Blink once”, at the top of the figure), 50th percentile (“Look down”, in the middle), and 10th percentile (“Bend neck to the right”, at the bottom) of the sample for  $k = 3$ . Hence, these examples represent the cases where the BCI is least, average, and most affected by noise, respectively.

In order to explain the results obtained, we created a ranking system where the first positions are those for which the average across columns  $k = 1, 2, 3$  is highest. The first position is then taken by the action “Do nothing” (as expected). In this case, the type of noise that is being added to the BCI data set is an EEG signal with no other source of contamination. Thus, it is reasonable that the performance of the simulated portable BCI is not largely affected by the addition of this artifact, even though different electrode impedances will result in differences in signal amplitude, since the data have not been normalized.

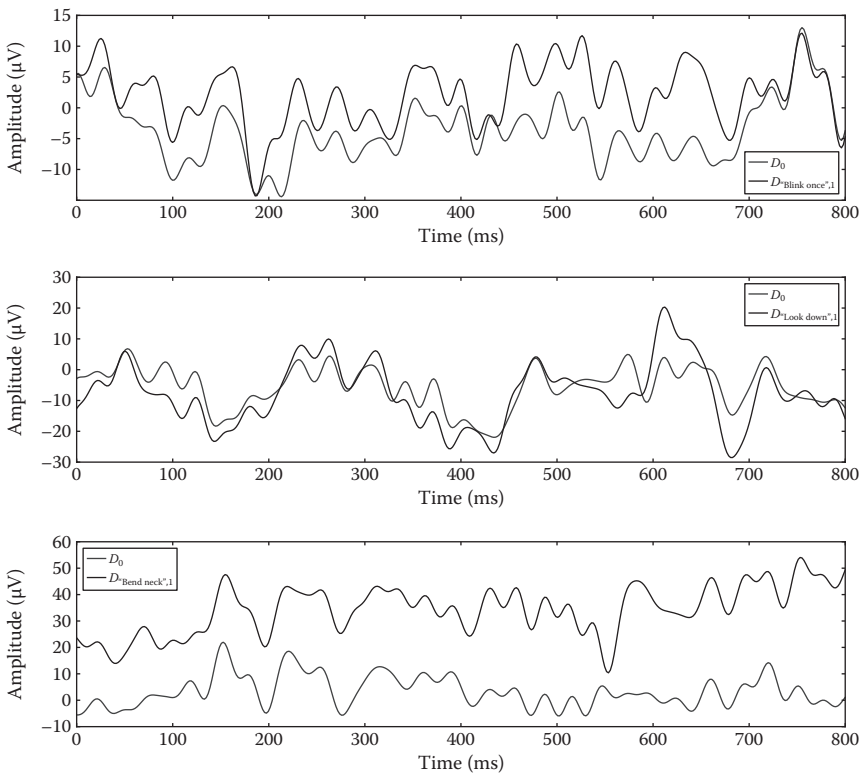


**FIGURE 9.5** Examples of epochs from  $D_0$  and  $D_{j,k}$ . Top: target trial with an eye blink at electrode site Cz; middle: target trial with an eye movement (“Look down”) at Cz; bottom: target trial with a neck movement (“Bend neck to the right”) at Oz.

Other artifacts that dominate the ranking are “Electrical noise” and “Squint”. Again, the contribution of these should not largely affect BCI performance, given that we are filtering the data above 40 Hz. Mains noise appears as a frequency component of 60 Hz, so our filter removes most of it. Similarly, EMG artifacts from muscle contractions, such as those produced by squinting, can be eliminated by low-pass filtering the signals above 30 Hz.

At the lower end of the ranking, we mostly find artifacts related to neck movements (e.g., those that involve bending or turning the neck). This is not an unexpected result for one main reason: during the data collection of artifacts, the volunteer had a head rest on the chair, so neck movements most likely also involved changes in electrode position, with associated sustained voltage shifts. This is clearly represented in [Figure 9.5](#) (bottom), even if the artifact epoch was preprocessed before adding it to the direction epoch. However, head rests are also available on a car; hence, the results obtained with our simulated portable BCI data sets are likely to be very similar to real data collected from a driver.

The last row of [Table 9.2](#) represents the average value of each column, so that the effects of increasing the interference of artifacts on the BCI data can be observed in this summary. As expected, performance decreases monotonically with increasing values of  $k$  (i.e., when more noise is present, the number of false positives and false negatives increases, and as a result, we obtain lower AUC values). Even though this decrease is not statistically significant for  $k = 1$  (only one type of artifact reaches statistical significance in this case), the effects of adding noise have a substantial impact on performance, as shown in the last column of the table, where for 24 out of the 25 types of artifacts (the only exception is the “Do nothing” activity, as expected), the performance of the BCI is significantly worse than in the ideal conditions of the BCI mouse experiment.

This raises the question of whether it is worth including some noisy trials when training the classifiers, once the types of artifacts that will later be encountered during the use of the portable BCI are known.

### 9.4.3 EFFECTS OF TRAINING WITH SIMULATED PORTABLE BCI DATA SETS

If one knows in advance the type of artifacts that are more common in a mobile application of a BCI, he or she could wonder whether it is better to include some noise of that type during training the classifier, in order to increase the robustness of the system, or if performance is better when the training set is composed only of data collected under ideal conditions.

In order to check this, we performed an extra experiment in which we trained and tested classifiers using data from the simulated portable BCI data sets only. In particular, for each tuple  $(j,k)$ , where  $j$  is the type of artifact and  $k$  is the number of occurrences of that type of artifact in each direction epoch (and, thus, gives an idea of the percentage of contamination in the data set), we trained classifier  $C_{p,j,k}$  with the training set of participant  $p$  from data set  $D_{j,k}$  and then calculated the individual AUC with the test set of that participant from the same data set. [Table 9.3](#) reports the median AUC across all participants obtained in this way. The numbers in brackets represent the result of a one-sided Wilcoxon test comparing the

**TABLE 9.3**  
**Performance of the BCI When Trained and Tested on the Simulated Mobile BCI Data Sets**

Noise Type	$k = 1$	$k = 2$	$k = 3$	Rank
Turn neck to the left	<b>0.742</b> (0.002)	<b>0.741</b> (0.007)	<b>0.708</b> (0.001)	21
Turn neck to the right	<i>0.747</i> (0.032)	<i>0.750</i> (0.041)	<b>0.710</b> (0.001)	20
Move head up	<b>0.716</b> (0.002)	<b>0.686</b> (0.000)	<b>0.668</b> (0.000)	25
Move head down	0.749 (0.052)	<b>0.735</b> (0.007)	<b>0.700</b> (0.001)	23
Move your tongue (mouth closed)	0.777 (0.164)	<i>0.769</i> (0.041)	<b>0.749</b> (0.003)	3
Move eyes to the left	0.777 (0.139)	<i>0.747</i> (0.032)	<i>0.760</i> (0.032)	6
Blink once	0.766 (0.065)	<i>0.744</i> (0.010)	<b>0.734</b> (0.002)	17
Blink repeatedly	0.769 (0.080)	<i>0.750</i> (0.010)	<b>0.738</b> (0.005)	14
Move eyes to the right	0.769 (0.097)	<i>0.753</i> (0.014)	<i>0.756</i> (0.020)	7
Look up	0.788 (0.287)	<b>0.729</b> (0.001)	<i>0.725</i> (0.010)	18
Look down	0.766 (0.065)	0.765 (0.052)	<b>0.747</b> (0.005)	9
Turn the wheel left	0.782 (0.171)	0.770 (0.139)	<i>0.766</i> (0.014)	1
Turn the wheel right	0.779 (0.145)	<i>0.738</i> (0.032)	<b>0.728</b> (0.001)	16
Change gear with left hand	0.775 (0.139)	<b>0.759</b> (0.007)	<i>0.755</i> (0.019)	4
Change gear with right hand	0.779 (0.164)	0.777 (0.117)	<i>0.754</i> (0.019)	2
Do nothing	0.780 (0.097)	<i>0.766</i> (0.041)	<b>0.739</b> (0.002)	5
Yawn	0.768 (0.221)	<b>0.733</b> (0.002)	<i>0.761</i> (0.041)	11
Swallow	0.766 (0.097)	<b>0.752</b> (0.005)	<b>0.742</b> (0.007)	12
Count in loud voice	<i>0.754</i> (0.032)	0.753 (0.052)	<b>0.734</b> (0.005)	19
Cross left foot over right	0.766 (0.080)	<i>0.751</i> (0.010)	<b>0.731</b> (0.002)	15
Cross right foot over left	0.775 (0.164)	<i>0.740</i> (0.010)	<i>0.762</i> (0.014)	8
Squint	0.777 (0.117)	<i>0.744</i> (0.010)	<i>0.737</i> (0.010)	13
Bend neck to the right	0.761 (0.117)	<b>0.687</b> (0.001)	<b>0.682</b> (0.000)	24
Bend neck to the left	0.759 (0.052)	<b>0.713</b> (0.003)	<b>0.713</b> (0.001)	22
Electrical noise	<i>0.761</i> (0.014)	<b>0.759</b> (0.007)	<b>0.749</b> (0.007)	10
Mean	0.766	0.744	0.734	

*Note:* Each number represents the median AUC across all participants for a specific type of artifact (from top to bottom,  $j = 1, \dots, 25$ ) and the given number of occurrences ( $k = 1, \dots, 3$ ). The last row represents the average AUC across data sets  $D_{j \in [1, 25], k}$ . Numbers in parentheses represent the  $p$  values of a one-sided Wilcoxon test comparing BCI performance of classifiers  $C_p$  when tested on  $D_0$  versus classifiers  $C_{p,j,k}$  tested on data sets  $D_{j,k}$ . Numbers in italics represent statistical significance at the 5% confidence level. Numbers in boldface represent statistical significance at the 1% confidence level. The last column represents the ranking table (low numbers represent higher AUCs) determined by the mean value across columns  $k = 1, 2, 3$ .

AUCs from classifiers  $C_{p,j,k}$  (described above) with those of the baseline case (from Section 9.4.1).

As in the previous case (Section 9.4.2), we expected the AUCs to drop significantly with respect to the baseline case, especially for larger values of  $k$ . Indeed, this result was replicated, and the  $p$  values reported in Table 9.3 show that the differences for this case versus the original BCI data are more statistically significant.

If we now compare [Table 9.3](#) with [Table 9.2](#), we see that the ranking column shows no differences in the last positions of the ranking, which are still dominated by neck movements. In general, the order of the ranking list is maintained across all artifacts. However, there are some types of artifacts for which large variations are registered. In particular, the main changes in the ranking order are given by eye movements (e.g., “Move eyes to the right”, “Look down”), which are now higher on the list than previously. Conversely, the main decreases on the ranking are given by eye blinks (both for one blink and several blinks). This suggests that this method is more robust to some types of artifacts than the one presented in Section 9.4.2. However, despite the changes in ranking order, the mean AUCs from which the rankings were calculated are still higher in [Table 9.2](#) (i.e., when the classifiers are trained using only BCI data).

To answer the question of whether training with artifact-contaminated data is more suitable for portable BCIs than training under ideal circumstances, we checked for significant differences between the results of [Table 9.2](#) versus [Table 9.3](#) with a one-sided paired Wilcoxon test (results not reported). According to this, the only case in which the latter is significantly worse than the former consistently across all values of  $k$  is the “Blink once” activity ( $p$  values for  $k = 1, 2, 3$  are 0.04, 0.039, and 0.02 respectively). Thus, despite the last row of both tables having such different mean values, it seems that (except when including blinks) training with noisy data will not affect the performance of the portable BCI during its use. Indeed, only in 4 out of the 25 types of artifacts was the difference between both methods significant for  $k = 3$ .

When taken together, all the evidence seems to point out that the first method of those presented (i.e., training with laboratory data) is either equal or significantly superior to the second, especially given the fact that eye blinks cannot be totally avoided during BCI use. However, when making this decision, one should also bear in mind that a lot of work has been done in terms of artifact correction methods for eye blinks.

## 9.5 CONCLUSIONS AND FUTURE WORK

BCIs have a great potential both in and outside of the laboratories. However, for this technology to work outside the ideal laboratory conditions, it is necessary to make it robust to artifacts and interferences.

Much of the noise that contaminates EEG data comes directly from the user in the form of EMG and EOG artifacts. Hence, for a portable BCI, it is important to characterize these and develop effective artifact correction methods that deal with them without affecting overall BCI performance and speed.

In this chapter, we ranked 25 types of artifacts on the basis of their effect on BCI performance decay. These included several forms of face muscular activity (e.g., squinting, blinking, and yawning) and neck, leg, and arm movements that are representative of actions that occur naturally while driving. Noise was artificially added to real BCI data from an Essex BCI Mouse experiment.

We analyzed the rankings in two different scenarios: one that simulates the action of training the BCI under ideal laboratory conditions and another that trains the

machine using artifact-contaminated data. Both systems were then tested on a noisy data set.

We showed that performance decreases with respect to ideal laboratory conditions, but the drop is not too severe, which allows for the use of portable BCIs. Furthermore, with respect to whether there is an advantage in purposefully contaminating the BCI training set with artifacts that will later be found on the move, our results suggest that this is a suboptimal approach. By adding noise to the training data set, the classifier is not able to learn the ground truth properly and, if given the same number of samples as in “ideal” conditions, performance overall will be lower during online use.

One of the main limitations of our work is the fact that artifacts were artificially added to the BCI data, rather than collected directly during a BCI experiment. One of the reasons for using this method was that it allowed for more control over the data set. The collection of artifacts took approximately 2 h, which would have been a very long time for a pure BCI experiment. Also, by collecting data separately, we could create a variety of data sets, which would not have been possible otherwise (because of contamination of neural signals caused by the BCI paradigm and the extremely long time that it would have taken). Moreover, if artifacts and BCI data are collected together, participants of the experiment are given a dual task, which would also have negatively affected BCI performance for the baseline case.

Another limitation is the fact that artifacts were collected with the volunteer in a seated position. While these results might be generalized to the cases where the user is driving or screening for targets within bursts of images, we have not studied the effects of standing (and possibly walking) on BCI performance. The type of BCI that we tested in this work is a P300-based BCI. However, our approach can be generalized to other types of BCI (e.g., motor imagery or steady-state visual evoked potentials) and other EEG purposes like those mentioned in Section 9.1. In most types of existing BCIs, the user needs some degree of sustained attention to control the system. Hence, for instance, a person will not be able to use a P300-based BCI while walking. However, for portable EEG monitoring and EEG-based wearables, the effects of leg motion artifacts still need to be studied.

Despite the limitations discussed above, our results show that the effects of several types of noise on BCI performance can be greatly diminished with appropriate filtering. Moreover, the algorithms that we used for data preprocessing are fast enough to allow for online (i.e., real time) use of the BCI. They are also suitable to be implemented in a portable BCI system, which we will test in the future. Furthermore, despite their simplicity, we have shown that, for low levels of contamination, the decrease of performance of the BCI was not significant with respect to ideal laboratory conditions.

## REFERENCES

1. Andrew B Schwartz. 2004. Cortical neural prosthetics. *Annual Review of Neuroscience*, 27:487–507.
2. Wilson Truccolo, Gerhard M Friehs, John P Donoghue, and Leigh R Hochberg. 2008. Primary motor cortex tuning to intended movement kinematics in humans with tetraplegia. *The Journal of Neuroscience: The Official Journal of the Society for Neuroscience*, 28(5):1163–1178, Jan.

3. Lawrence A Farwell and Emanuel Donchin. 1988. Talking off the top of your head: Toward a mental prosthesis utilizing event-related brain potentials. *Electroencephalography and Clinical Neurophysiology*, 70(6):510–523, Dec.
4. Jonathan R Wolpaw, Dennis J McFarland, Gregory W Neat, and Catherine A Forneris. 1991. An EEG-based brain–computer interface for cursor control. *Electroencephalography and Clinical Neurophysiology*, 78(3):252–259, Mar.
5. Gert Pfurtscheller, Doris Flotzinger, and Joachim Kalcher. 1993. Brain–computer interface: A new communication device for handicapped persons. *Journal of Microcomputer Applications*, 16(3):293–299.
6. Niels Birbaumer, Nimr Ghanayim, Thilo Hinterberger, Iver Iversen, Boris Kotchoubey, Andrea Kübler, Jouri Perelmouter, Edward Taub, and Herta Flor. 1999. A spelling device for the paralysed. *Nature*, 398(6725):297–298, Mar.
7. Nikolaus Weiskopf, Klaus Mathiak, Simon W Bock, Frank Scharnowski, Ralf Veit, Wolfgang Grodd, Rainer Goebel, and Niels Birbaumer. 2004. Principles of a brain–computer interface (BCI) based on real-time functional magnetic resonance imaging (fMRI). *IEEE Transactions on Biomedical Engineering*, 51(6):966–970, June.
8. Jonathan R Wolpaw and Dennis J McFarland. 2004. Control of a two-dimensional movement signal by a noninvasive brain–computer interface in humans. *Proceedings of the National Academy of Sciences of the U.S.A.*, 101(51):17849–17854, Dec.
9. Eric W Sellers and Emanuel Donchin. 2006. A P300-based brain–computer interface: Initial tests by ALS patients. *Clinical Neurophysiology*, 117(3):538–548, Mar.
10. Guido Dornhege, José del R Millán, Thilo Hinterberger, Dennis J McFarland, and Klaus-Robert Müller, editors. 2007. *Toward Brain-Computer Interfacing*. MIT Press, Cambridge, Massachusetts.
11. Roman Krepki, Gabriel Curio, Benjamin Blankertz, and Klaus-Robert Müller. 2007. Berlin brain–computer interface—The HCI communication channel for discovery. *International Journal of Human-Computer Studies*, 65(5):460–477.
12. Niels Birbaumer, Andrea Kübler, Nimr Ghanayim, Thilo Hinterberger, Jouri Perelmouter, Jochen Kaiser, Iver Iversen, Boris Kotchoubey, Nicola Neumann, and Herta Flor. 2000. The thought translation device (TTD) for completely paralyzed patients. *IEEE Transactions on Rehabilitation Engineering*, 8(2):191.
13. Jonathan R Wolpaw, Niels Birbaumer, William J Heetderks, Dennis J McFarland, P Hunter Peckham, Gerwin Schalk, Emanuel Donchin, Louis A Quatrano, Charles J Robinson, and Theresa M Vaughan. 2000. Brain–computer interface technology: A review of the first international meeting. *IEEE Transactions on Rehabilitation Engineering*, 8(2):164–173, June.
14. Mathew Salvaris, Caterina Cinel, Luca Citi, and Riccardo Poli. 2012. Novel protocols for P300-based brain–computer interfaces. *IEEE Transactions on Neural Systems and Rehabilitation Engineering*, 20(1):8–17.
15. Luca Citi, Riccardo Poli, Caterina. Cinel, and Francisco Sepulveda. 2008. P300-based BCI mouse with genetically-optimized analogue control. *IEEE Transactions on Neural Systems and Rehabilitation Engineering*, 16(1):51–61, Feb.
16. José del Ramón Millán, Rüdiger Rupp, Gernot R Müller-Putz, Roderick Murray-Smith, Claudio Giugliemma, Michael Tangermann, Carmen Vidaurre, Febo Cincotti, Andrea Kübler, Robert Leeb, Christa Neuper, Klaus-Robert Müller and Donatella Mattia. 2010. Combining brain–computer interfaces and assistive technologies: State-of-the-art and challenges. *Frontiers in Neuroscience*, (4):161. doi:10.3389/fnins.2010.00161.
17. Chin-Teng Lin, Hung-Yi Hsieh, Sheng-Fu Liang, Yu-Chieh Chen, and Li-Wei Ko. 2007. Development of a wireless embedded brain–computer interface and its application on drowsiness detection and warning. In Don Harris, editor, *Engineering Psychology and Cognitive Ergonomics*, volume 4562 of *Lecture Notes in Computer Science*, pages 561–567. Springer Berlin Heidelberg.

18. Danny Plass-Oude Bos, Boris Reuderink, Bram Laar, Hayrettin Grkk, Christian Mhl, Mannes Poel, Anton Nijholt, and Dirk Heylen. 2010. Brain-computer interfacing and games. In Desney S Tan and Anton Nijholt, editors, *Brain-Computer Interfaces, Human-Computer Interaction Series*, pages 149–178, Springer London.
19. Maria V Ruiz Blondet, Adarsha Badarinath, Chetan Khanna, and Zhanpeng Jin. 2013. A wearable real-time BCI system based on mobile cloud computing. In *Neural Engineering (NER), 2013 6th International IEEE/EMBS Conference on*, pages 739–742, San Diego, CA, Nov.
20. Mohammad Modarreszadeh and Robert N Schmidt. 1997. Wireless, 32-channel, EEG and epilepsy monitoring system. In *Engineering in Medicine and Biology Society, 1997. Proceedings of the 19th Annual International Conference of the IEEE*, volume 3, pages 1157–1160, Chicago, Oct.
21. Lars Torsvall, Torbjurn Akerstedt, Katja Gillander, and Anders Knutsson. 1989. Sleep on the night shift: 24-hour EEG monitoring of spontaneous sleep/wake behavior. *Psychophysiology*, 26(3):352–358.
22. David J Kupfer, F. Gordon Foster, Patricia Coble, Richard J McPartland, and Richard F Ulrich. 1978. The application of EEG sleep for the differential diagnosis of affective disorders. *American Journal of Psychiatry*, 135(1):69–74.
23. Ana Matran-Fernandez, Riccardo Poli, and Caterina Cinel. 2013. Collaborative brain-computer interfaces for the automatic classification of images. In *Neural Engineering (NER), 2013 6th International IEEE/EMBS Conference on*, pages 1096–1099, San Diego (CA), Nov 6–8, IEEE.
24. Ana Matran-Fernandez and Riccardo Poli. 2014. Collaborative brain-computer interfaces for target localisation in rapid serial visual presentation. In *Computer Science and Electronic Engineering Conference (CEEC), 2014 6th*, pages 127–132, Colchester, September 25–26 2014, IEEE.
25. Riccardo Poli, Davide Valeriani, and Caterina Cinel. 2014. Collaborative brain-computer interface for aiding decision-making. *PLoS ONE*, 9(7):e102693.
26. Todd C. Handy, editor. 2004. *Event-Related Potentials. A Method Handbook*. MIT Press, Cambridge, Massachusetts.
27. Steven J. Luck. 2005. *An Introduction to the Event-Related Potential Technique*. MIT Press, Cambridge, Massachusetts.
28. Riccardo Poli, Luca Citi, Francisco Sepulveda, and Caterina Cinel. 2009. Analogue evolutionary brain computer interfaces. *IEEE Computational Intelligence Magazine*, 4(4):27–31, Nov.
29. Mathew Salvaris, Caterina Cinel, Riccardo Poli, Luca Citi, and Francisco Sepulveda. 2010. Exploring multiple protocols for a brain-computer interface mouse. In *Proceedings of 32nd IEEE EMBS Conference*, pages 4189–4192, Buenos Aires, Sept.
30. Mehrdad Fatourehchi, Ali Bashashati, Rabab K Ward, and Gary E Birch. 2007. EMG and EOG artifacts in brain computer interface systems: A survey. *Clinical Neurophysiology*, 118(3):480–494.
31. Rolf Verleger, Theo Gasser, and Joachim Möcks. 1982. Correction of EOG artifacts in event-related potentials of the EEG: Aspects of reliability and validity. *Psychophysiology*, 19(4):472–480, July.
32. Steven J Luck. 2014. *An Introduction to the Event-Related Potential Technique*. MIT Press, Cambridge, Massachusetts.
33. Aapo Hyvärinen, Juha Karhunen, and Erkki Oja. 2001. *Independent Component Analysis*. New York, Wiley-IEEE.
34. Scott Makeig, Anthony J. Bell, Tzyy-Ping Jung, and Terrence J. Sejnowski. 1996. Independent component analysis of electroencephalographic data. In David S. Touretzky, Michael C. Mozer, and Michael E. Hasselmo, editors, *Advances in Neural Information Processing Systems*, volume 8, pages 145–151, MIT Press, Cambridge, Massachusetts.

35. Scott Makeig, Marissa Westerfield, Tzzy-Ping Jung, James Covington, Jeanne Townsend, Terrence J Sejnowski, and Eric Courchesne. 1999. Functionally independent components of the late positive event-related potential during visual spatial attention. *The Journal of Neuroscience*, 19(7):2665–2680, Apr.
36. Tzzy-Ping Jung, Scott Makeig, Marissa Westerfield, Jeanne Townsend, Eric Courchesne, and Terrence J Sejnowski. 2001. Analysis and visualization of single-trial event-related potentials. *Human Brain Mapping*, 14(3):166–185, Nov.
37. Scott Makeig, Marissa Westerfield, Tzzy-Ping Jung, S Enghoff, Jeanne Townsend, Eric Courchesne, and Terrence J Sejnowski. 2002. Dynamic brain sources of visual evoked responses. *Science (New York, N.Y.)*, 295(5555):690–694, Jan.
38. Hugh Nolan, Robert Whelan, and Richard B Reilly. 2010. FASTER: Fully automated statistical thresholding for EEG artifact rejection. *Journal of Neuroscience Methods*, 192(1):152–162, Sept.
39. Jessica D Bayliss and Dana H Ballard. 1999. Single trial P300 recognition in a virtual environment. In *Proceedings of the International Congress on Computational Intelligence: Methods & Applications*, June 22–25, Rochester, New York, USA. ICSC Academic Press.
40. Rodney J Croft and Robert J Barry. 2000. Removal of ocular artifact from the EEG: A review. *Clinical Neurophysiology*, 30:5–19.
41. Markus Junghöfer, Thomas Elbert, Don M Tucker, and Brigitte Rockstroh. 2000. Statistical control of artifacts in dense array EEG/MEG studies. *Psychophysiology*, 37:523–532.
42. Daniel Göhring, David Latotzky, Miao Wang, and Raúl Rojas. 2013. Semi-autonomous car control using brain computer interfaces. In Sukhan Lee, Hyungsuck Cho, Kwang-Joon Yoon and Jangmyung Lee, editors, *Intelligent Autonomous Systems 12*, pages 393–408, Berlin, Springer.
43. Riccardo Poli, Caterina Cinel, Ana Matran-Fernandez, Francisco Sepulveda, and Adrian Stoica. 2013. Towards cooperative brain–computer interfaces for space navigation. In *Proceedings of the 2013 International Conference on Intelligent User Interfaces*, pages 149–160, Santa Monica, CA, ACM, March.

